Letter to the Editor

Effect of smoothening functions on the frequency response of an oscillator with clearance non-linearity

T.C. Kim, T.E. Rook, R. Singh*

Acoustics and Dynamics Laboratory, Department of Mechanical Engineering and The Center for Automotive Research, The Ohio State University, 206 West 18th Avenue, Columbus, OH 43210-1107, USA

1. Introduction

Fig. 1(a) describes a generic clearance type stiffness non-linearity $f(\delta)$. Only a symmetric function with two stages is considered though one could easily generalize the concepts of this article. Mathematically, $f(\delta)$ can be described over three piecewise linear regimes as follows where $0 \leqslant \alpha \leqslant 1$, and can be written as below using the absolute function $g(\delta \mp b) = |\delta \mp b|$:

$$f(\delta) = \begin{cases} \delta - (1 - \alpha)b, & b < \delta, \\ \alpha\delta, & -b \leqslant \delta \leqslant b, \\ \delta + (1 - \alpha)b, & \delta < -b, \end{cases}$$
$$= \delta + (1 - \alpha)\frac{g(\delta - b) - g(\delta + b)}{2}. \tag{1}$$

Further, one can rewrite the *signum* or *sgn* function in terms of derivative of the absolute function $g(\delta \mp b)$ as below where superscript $'$ implies a derivative with respect to δ:

$$\text{sgn}(\delta \mp b) = \mathrm{d}|\delta \mp b|/\mathrm{d}\delta = g'(\delta \mp b). \tag{2}$$

The reason for investigating the $g'(\delta \mp b)$ term separately is that the sgn function is used when the frictional hysteresis is described along with the non-linear stiffness function. Accordingly, modify $f(\delta)$ to define $f(\delta, \dot{\delta})$ that will include velocity related frictional hysteresis terms $f_H(\delta, \dot{\delta})$. Here, the relative velocity is defined as $\dot{\delta} = \mathrm{d}\delta/\mathrm{d}t$. As shown in Fig. 1(b), when $\dot{\delta} > 0$, the $f_H(\delta, \dot{\delta})$ term follows the upper locus drawn by a "dash-dot" line, and an increase in δ results in an abrupt jump in force at b, from the hysteresis value H_1 to H_2. When $\dot{\delta} < 0$, the $f_H(\delta, \dot{\delta})$ term follows the lower locus, the "dashed" line. Now, the jump takes place at $-b$ from H_1 to H_2. The $f_H(\delta, \dot{\delta})$ function

---

*Corresponding author. Tel.: +1-614-292-9044; fax: +1-614-292-3163.

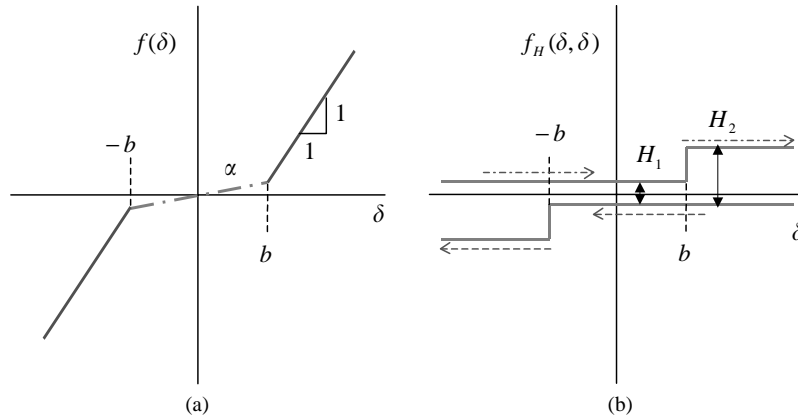*E-mail address:* singh.3@osu.edu (R. Singh).

Fig. 1. Non-linear functions with discontinuities. (a) Clearance non-linear stiffness function $f(\delta)$ with slopes of α and 1 over the piecewise linear regimes; (b) frictional hysteresis function $f_H(\delta, \dot{\delta})$ with dual values H_1 and H_2.

depends only on the sign of $\dot{\delta}$ and the $\delta \pm b$ value. Mathematically, it is written as follows:

$$f_H(\delta, \dot{\delta}) = \text{sgn}(\dot{\delta})\frac{H_2}{2} + \frac{(H_2 - H_1)}{4}[\text{sgn}(\delta + b)(1 - \text{sgn}(\dot{\delta})) + \text{sgn}(\delta - b)(1 + \text{sgn}(\dot{\delta}))]$$

$$= g'(\dot{\delta})\frac{H_2}{2} + \frac{(H_2 - H_1)}{4}[g'(\delta + b)(1 - g'(\dot{\delta})) + g'(\delta - b)(1 + g'(\dot{\delta}))]. \tag{3}$$

Note that $f(\delta)$ or $f(\delta, \dot{\delta})$ describes a non-analytical, non-differential and discontinuous function. This would obviously pose problems in numerical simulations, especially around the stiffness transitions at $\pm b$ [1–7]. In this communication, we present several smoothening functions and demonstrate their influence on the non-linear frequency response characteristics of a single-degree-of-freedom system. Responses at the primary as well as super-harmonics are considered given sinusoidal excitation.

2. Smoothening functions

The absolute and the sgn functions of Eqs. (1)–(3) can be smoothened using the trigonometric or polynomial type functions and a regularizing factor σ that can be adjusted to suit the needs of non-linear analysis. Technically, we are approximating the absolute (abs) function since the $\text{abs}(\delta) = \delta(\text{d}(\text{abs}(\delta))/\text{d}\delta)$ within the $(-b, \ b)$ regime. Even the $\alpha = 0$ value in Eq. (1) produces a piecewise continuous curve, but their derivatives are discontinuous (C^0 continuous). The sgn function only affects the derivatives of choice but is still bounded even though it is discontinuous. When replacing sgn with any smoothening function, one must consider its derivatives when describing the dynamic motion of an oscillator with dry friction. This is because the dry friction is discontinuous and the derivative is not bounded unless we describe it using tanh or arctan.

One can approximate Eqs. (2) and (3) with alternate smoothening functions where $\bar{g}_i(x)$ represents an approximation or estimation of the absolute function where $x = \delta \mp b$. Further, derivatives of $\bar{g}_i$ with respect to δ are described where superscripts $'$ and $''$ imply first and second

derivatives, respectively. Some of the more reliable smoothening functions are classified as follows.

1. Hyperbolic-tangent type

$$\hat{g}_1(x) = x \tanh(\sigma x), \tag{4a}$$

$$\hat{g}_1'(x) = \tanh(\sigma x) + x(1 - \tanh(\sigma x)^2)\sigma, \tag{4b}$$

$$\hat{g}_1''(x) = 2(1 - \tanh(\sigma x)^2)\sigma + x(2\tanh(\sigma x)(1 - \tanh(\sigma x)^2)\sigma^2). \tag{4c}$$

2. Arc-tangent type

$$\hat{g}_2(x) = x\frac{2}{\pi}\arctan(\sigma x), \tag{5a}$$

$$\hat{g}_2'(x) = \frac{2}{\pi}\arctan(\sigma x) + x\frac{2\sigma}{\pi(1 + (\sigma x)^2)}, \tag{5b}$$

$$\hat{g}_2''(x) = \frac{4\sigma}{\pi(1 + (\sigma x)^2)} + 4x\frac{\sigma^3 x}{\pi(1 + (\sigma x)^2)^2}. \tag{5c}$$

3. Hyperbolic-cosine type

$$\hat{g}_3(x) = \frac{1}{\sigma}\ln(2\cosh(\sigma x)), \tag{6a}$$

$$\hat{g}_3'(x) = \tanh(\sigma x), \tag{6b}$$

$$\hat{g}_3''(x) = \sigma - \tanh(\sigma x)^2\sigma. \tag{6c}$$

4. Quintic spline type (here, $y \equiv x/\varepsilon$ and where $\varepsilon = b/\sigma$)

$$\hat{g}_4(x) = \begin{cases} \frac{\varepsilon}{8}(3 + 6y^2 - 1y^4), & |y| \leqslant 1, \\ |x|, & |y| > 1. \end{cases} \tag{7a}$$

$$\hat{g}_4'(x) = \begin{cases} \frac{1}{8}(12y - 4y^3), & |y| \leqslant 1, \\ \text{sgn}(x), & |y| > 1. \end{cases} \tag{7b}$$

$$\hat{g}_4''(x) = \begin{cases} \frac{1}{8\varepsilon}(12 - 12y^2), & |y| \leqslant 1, \\ 0, & |y| > 1. \end{cases} \tag{7c}$$

Yet for both numerical and semi-analytical simulation schemes, the effect of σ is not fully understood and its lower limit has not yet been tested [4–7]. A smaller σ value is desirable as it will

decrease the calculation time and increase convergence of simulation codes. The larger the σ value, the closer is the approximated $\bar{g}_i$ curve to the original non-linear function. A very high value of σ (such as 10^6) seems to work well in some numerical simulations [3–6], but this can cause numerical instability since it has enormous influence on the response, especially when α is near zero. Consequently finer integration time steps are needed so that the algorithm can adapt itself to very abrupt changes in the non-linear function.

3. Comparison of functions

Fig. 2 compares the smoothening functions described above with $\alpha = 0.0$, $b = 0.1745$ and $\sigma = 250$. In particular, the quintic spline $\bar{g}_4$ type does not convert the non-linear function of Eq. (2) into a globally continuous single function (across the whole domain) like $\bar{g}_1$, $\bar{g}_2$ and $\bar{g}_3$. Instead, $\bar{g}_4$ requires calculation of proximity values $\pm \varepsilon$ based on σ, and smoothens only the localized regime between $\pm \varepsilon$. For the spline, we do not scale the x-axis, instead we define the different regions of the x-axis. The approximation $\bar{g}_4$ provides continuous derivatives (as shown in Fig. 2(b)) and provides better accuracy in the vicinity of discontinuous non-linearities. This scheme can be effectively integrated in semi-analytical methods such as the harmonic balance method [8] and the shooting (numerical integration) method [9] with some modifications. The reason that this localized smoothening is effective is that the harmonic balance method involves sampling the non-linear function and its first derivative at evenly spaced a priori known time points without a need to find the exact transition points unlike numerical integration schemes. In contrast, the shooting method or numerical integration requires evaluating the function and its first derivative at unevenly spaced, non-a priori known time points which may in fact also require evaluations at the exact transition point. Numerical integration does not care about the particular kind of the smoothening functions; rather it cares about the continuity of the non-linear function itself. For example, the quintic spline function $\bar{g}_4$ is adapted in commercial software like ADAMS to speed up the numerical integration [7]. In contrast, the harmonic balance method gains its advantages at computation time and resources when evaluating non-linear functions [8] since this method avoids the calculation of the non-linear transitions. Next $\bar{g}_2$ appears to be a biased approximation of $g(\delta) \equiv |\delta|$ throughout the full range of δ (see Fig. 2(a)), even when a higher value of σ (such as 10^4) is applied. Conversely, $\bar{g}_1$, $\bar{g}_3$ and $\bar{g}_4$ are well-behaved. In fact, their first derivatives, $\bar{g}_1'$ and $\bar{g}_3'$, seem to resemble the step response of a first order system with a finite time constant (equal to σ). This can be expressed as $\bar{g}_{5+}' = 1 - e^{-\sigma x}$ for the positive side, and $\bar{g}_{5-}' = -1 + e^{\sigma x}$ for the negative side as shown in Fig. 2(b). However, our numerical simulations of the non-linear oscillator (with frictional hysteresis) confirm that a numerical overflow leading to a convergence problem is observed with "hyperbolic-cosine" approximation $\bar{g}_3$. This is because when only the sgn function is involved, simply saying $\text{sgn}(x) = \text{abs}(x)/x$ is not strictly correct, since $\text{abs}(x)/x$ is not defined at $x = 0$. Consequently, one must instead use $\text{sgn}(x) = \partial |x|/\partial x = g'(x)$ and the numerical singularity can be avoided. In this way, the derivative of the sgn function can be defined in all smoothening functions as shown in Fig. 2(c). Therefore, application of $\bar{g}_3$ should be performed with great care. It should be also noted that there does not exist a unique σ value that will work for all of the smoothening functions.
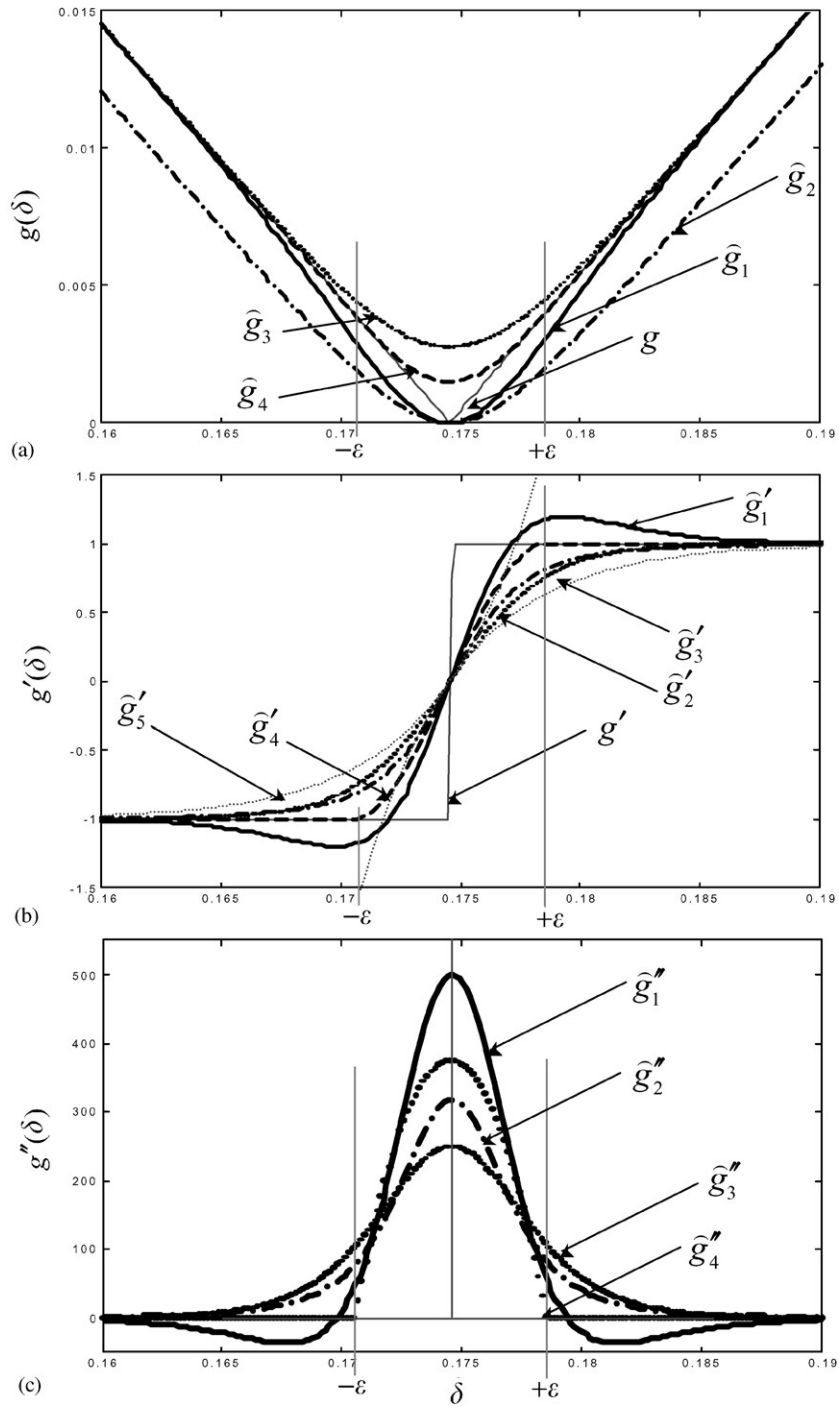
Fig. 2. Comparison of selected smoothening functions $\bar{g}_i$ and their derivatives given $b = 0.1745$ and $\sigma = 250$. (a) $\bar{g}_i(\delta - b)$; (b) $\partial \bar{g}_i(\delta - b)/\partial \delta$; (c) $\partial^2 \bar{g}_i(\delta - b)/\partial \delta^2$. (–) $\bar{g}_1$; (—) $\bar{g}_2$; ($\bigcirc$) $\bar{g}_3$; (– –) $\bar{g}_4$; ($\cdots\cdots$) $\bar{g}'_{5+} = 1 - e^{-\sigma x}$ and $\bar{g}'_{5-} = -1 + e^{\sigma x}$.

4. Non-linear responses

Now, consider a single-degree-of-freedom non-linear system with pure harmonic excitation at frequency ω_p (in the units of rad/s) under the influence of a mean force F_m:

$$\ddot{\delta} + 2\zeta_1\omega_1\dot{\delta} + \omega_1^2 f(\delta) = F_m + F_p \sin(\omega_p t + \varphi). \tag{8}$$

Here, ω_1 is the natural frequency (rad/s) corresponding to the second stage (with unity slope) of Fig. 1, ζ_1 is the corresponding damping ratio and F_p is the dynamic force amplitude. The steady
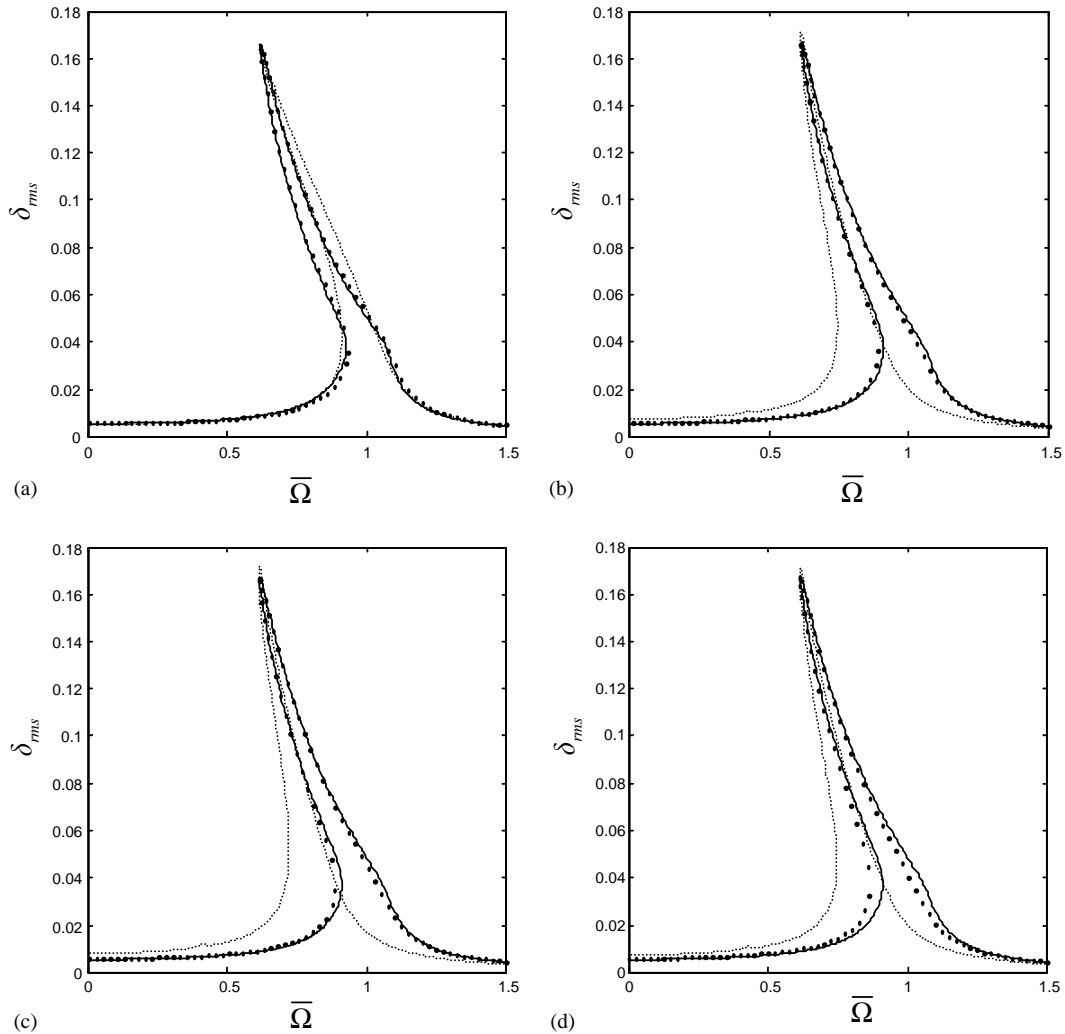

Fig 3. Effect of the smoothening factor σ on the response (with $n_{max} = 12$) for case 1 with $\alpha = 0.00$. (a) $\bar{g}_1$; (b) $\bar{g}_2$; (c) $\bar{g}_3$; (d) $\bar{g}_4$. (–) $\sigma = 100$; (○) $\sigma = 50$; (· · · · ·) $\sigma = 10$.

state response is assumed to be periodic with fundamental frequency ω_p:

$$\delta(t) = \delta_m + \sum_{n=1}^{n_{max}} \delta_{pn} \sin(n\omega_p t + \varphi_n), \tag{9}$$

where n is the harmonic index, n_{max} is the highest harmonic to be included, δ_m is the mean displacement, δ_{pn} is the harmonic amplitude and φ_n is the harmonic phase. We will consider 12 harmonics ($n_{max} = 12$) for all examples of this paper. A multi-term harmonic balance method is used to implement Eqs. (8) and (9) and construct the non-linear frequency response characteristics; this will be fully described in a future article [8]. Our semi-analytical approach matches well with numerical simulation and experiments.
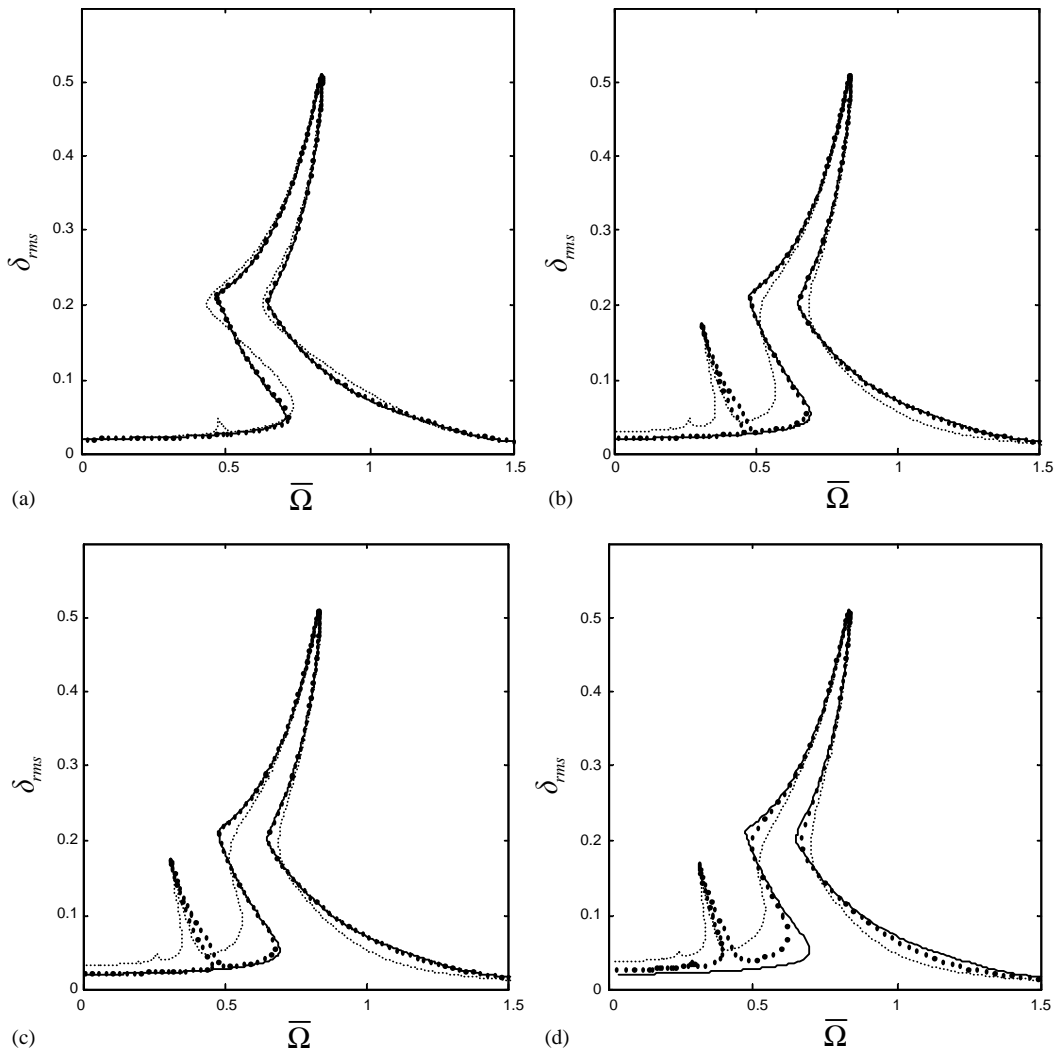

Fig 4. Effect of the smoothening factor σ on the response (with $n_{max} = 12$) for case 2 with $\alpha = 0.00$. (a) $\bar{g}_1$; (b) $\bar{g}_2$; (c) $\bar{g}_3$; (d) $\bar{g}_4$. (–), $\sigma = 100$; (○) $\sigma = 50$; ($\cdots\cdots$) $\sigma = 10$.

First, consider a case (designated as 1) that produces single-sided impacts given $\omega_1 = 1$, $\zeta_1 = 0.025$, $F_m = 0.05$, $F_p = 0.008$, and $b = 0.1745$. For this case with $\alpha = 0.0$, Fig. 3 shows typical non-linear frequency response characteristics in terms of $\delta_{r.m.s.}$ versus $\bar{\Omega} = \omega_p / \omega_1$, where $\delta_{r.m.s.}$ is the root-mean-square value of response. A noticeable drop in response is observed when $\sigma \leqslant 50$. In particular, when $\sigma = 10$, the transition point between multi-stiffness regimes can no longer be recognized, and the softening type single-sided impact response is not observed. The reliability of this analysis drops severely with the $\bar{g}_2$, $\bar{g}_3$, or $\bar{g}_4$ function, especially for the primary resonance and super-harmonic regimes. Conversely, $\bar{g}_1$ is accurate over all frequency spans without any sign of a super-harmonic dimple as found in other approximations. When $\sigma \geqslant 50$, the stiffness
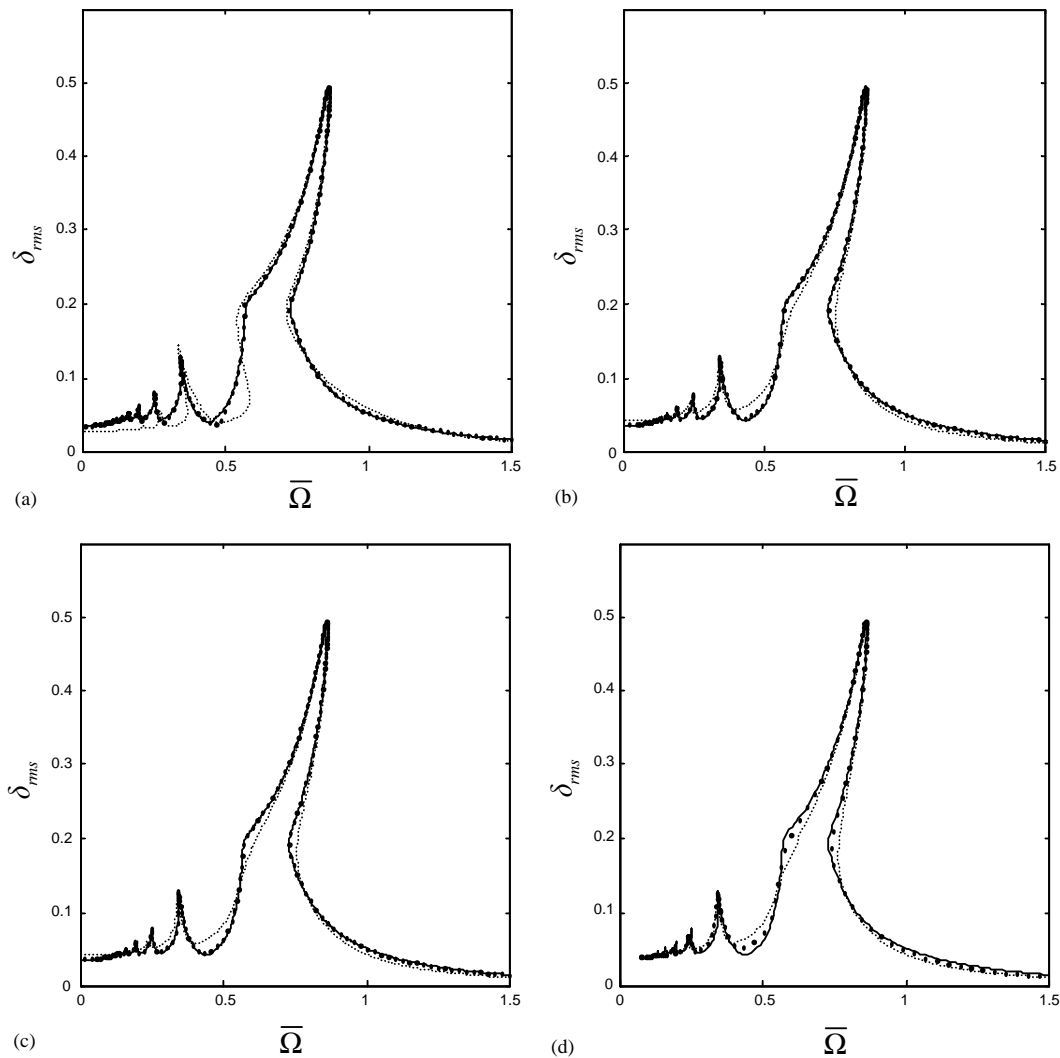

Fig. 5. Effect of the smoothening factor σ on the response (with $n_{max} = 12$) for case 2 with $\alpha = 0.18$. (a) $\bar{g}_1$; (b) $\bar{g}_2$; (c) $\bar{g}_3$; (d) $\bar{g}_4$. (–) $\sigma = 100$; ($\bigcirc$) $\sigma = 50$; ($\cdots\cdots$) $\sigma = 10$.
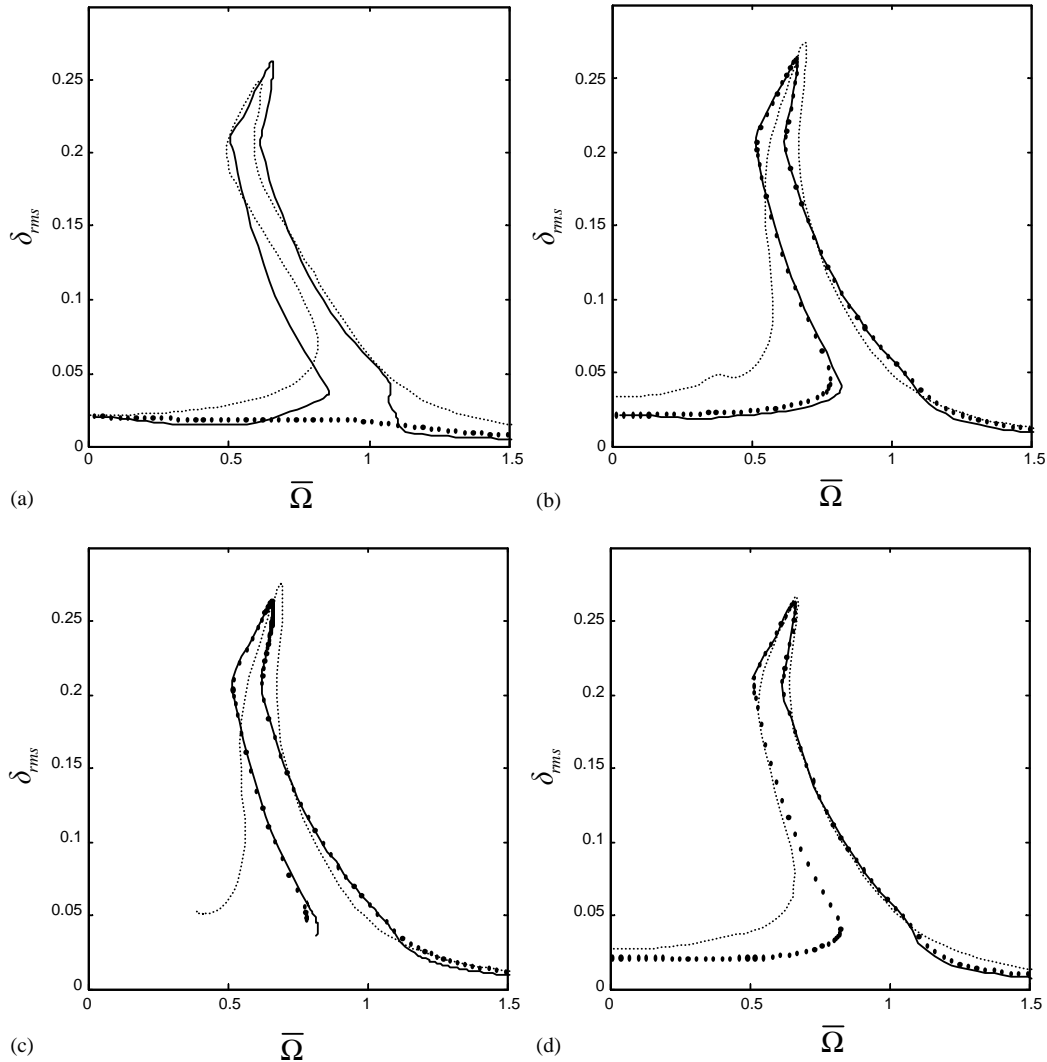
Fig. 6. Effect of the smoothening factor σ on the response (with $n_{max} = 12$) for case 2 with $\alpha = 0.00$, $H_1 = 0.005$, and $H_2 = 0.02$. (a) $\bar{g}_1$; (b) $\bar{g}_2$; (c) $\bar{g}_3$; (d) $\bar{g}_4$. (–) $\sigma = 100$; ($\bigcirc$) $\sigma = 50$; ($\cdots\cdots$) $\sigma = 10$.

transition regime is recognizable though it yields a very smooth curve. Nonetheless, even lower σ values can predict peak $\delta_{r.m.s.}$ values within a 5% error band. For the single-sided impact case, $\sigma \geqslant 50$ predicts reasonably accurate stiffness transition points and the overall dynamic response is reliably constructed.

   The same tendency is observed for the double-sided impact (case 2) with $\omega_1 = 1$, $\zeta_1 = 0.025$, $F_m = 0.05$, $F_p = 0.03$, and $b = 0.1745$. Fig. 4 shows the effect of σ with $\alpha = 0.00$. When $\sigma = 10$, the stiffness transition regimes appear too well rounded. This is especially true when a transition from single-sided to double-sided impact regimes takes place. Significant differences between $\sigma = 10$ and 100 cases are observed in both $\bar{\Omega}$ and $\delta_{r.m.s.}$ values as seen in Figs. 3–6. Some spurious super-
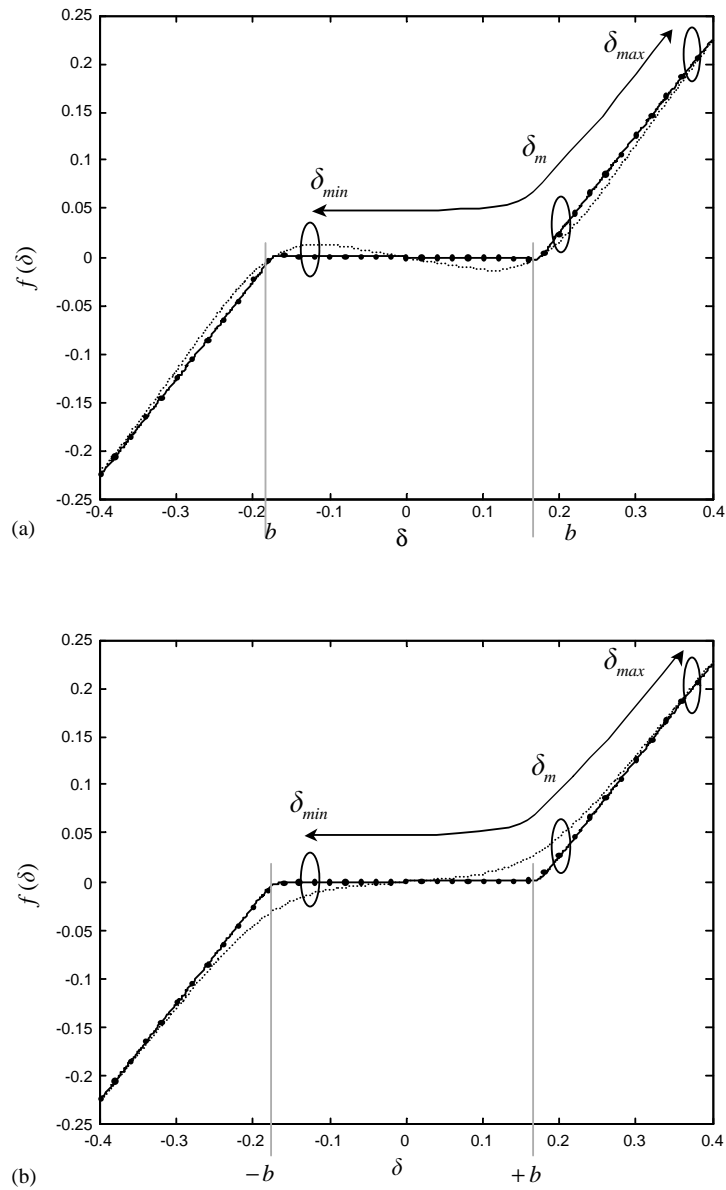
Fig 7. Effect of the smoothening factor σ on the non-linear function $f(\delta)$ for case 2 with $\alpha = 0.00$. Calculated displacements are $\delta_{min} = -0.1106$, $\delta_m = 0.2061$, and $\delta_{max} = 0.3821$. (a) With $\bar{g}_1(\delta)$; (b) with $\bar{g}_2(\delta)$. (–) $\sigma = 100$; (○) $\sigma = 50$; (· · · · ·) $\sigma = 10$.

harmonic peaks appear in Fig. 4 at $\bar{\Omega} = 0.48$ with $\sigma = 10$ for all smoothening approximations. But for $\sigma \geqslant 50$, no super-harmonic peaks are observed and the associated errors are within 2% for $\bar{g}_1$, though other functions still show spurious super-harmonic peaks. The spurious peak with $\sigma = 10$ is due to an incorrect representation of the clearance non-linearity as explained by Fig. 7. Clear differences between $\bar{g}_1$ and the other functions under the dynamic conditions are observed
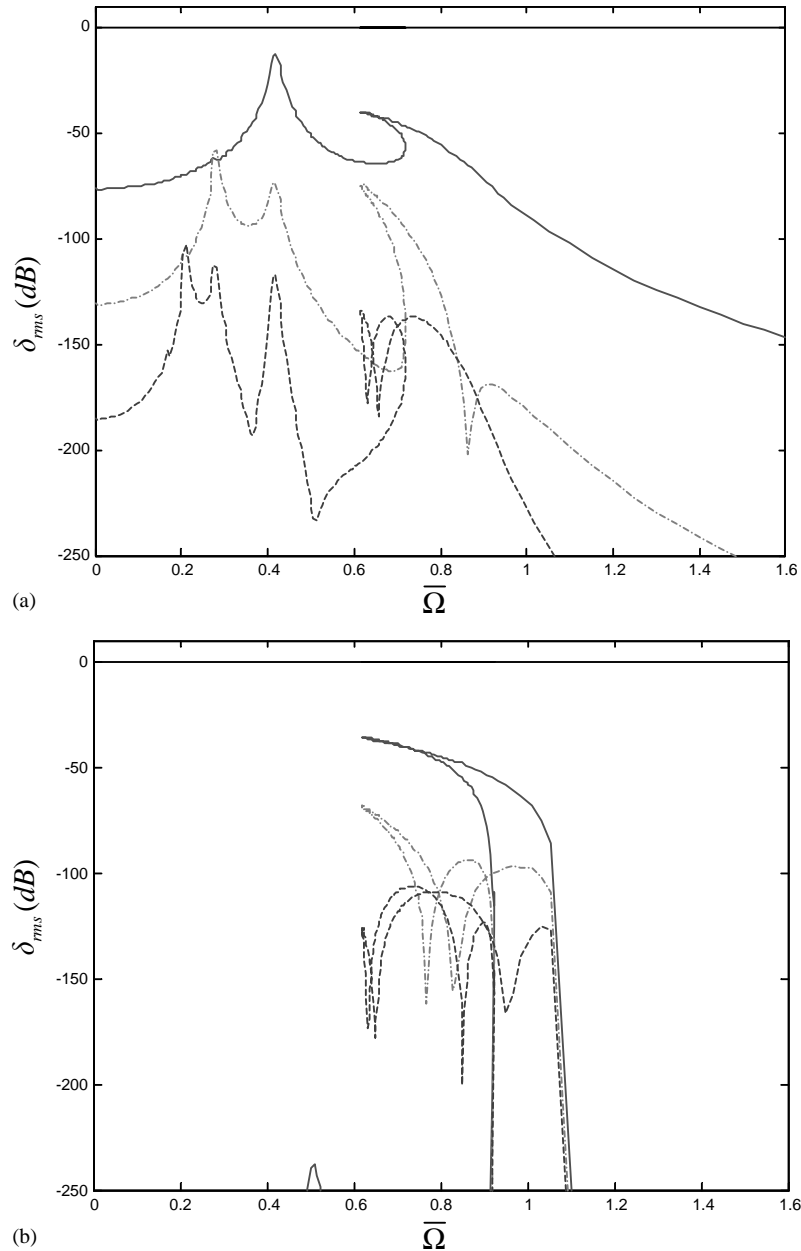
Fig. 8. Relative harmonic amplitudes of the periodic response (with $n_{max} = 12$) for case 1 with $\bar{g}_1$ and $\alpha = 0.000$. (a) $\sigma = 10$; (b) $\sigma = 50$. (–) Second harmonic ($n = 2$); (–) third harmonic ($n = 3$); (– –) fourth harmonic ($n = 4$). All dB values are with reference to the fundamental harmonic response.

in Figs. 3–6. Nevertheless, all smoothening approximations yield the same results when σ exceeds 50. The lower the σ value, the rounder the stiffness transition regime and a sufficiently small σ value can even produce the continuous non-linearity with $k_1 x \pm k_2 x^2 \pm k_3 x^3$ type terms. Fig. 8

compares the relative amplitudes of higher harmonics. Note that higher values of σ require a virtually infinite number of harmonics to truly construct the discontinuous non-linearity, based on the application of Gibb's phenomenon. Conversely, any $\bar{g}_i$ approximation with a lower σ can be easily represented by the first few harmonics. As seen in Fig. 8, the lower σ value yields larger second harmonic components. However, the peak $\delta_{r.m.s.}$ values at the primary resonance remain the same even with lower σ values as seen in Figs. 3–6.
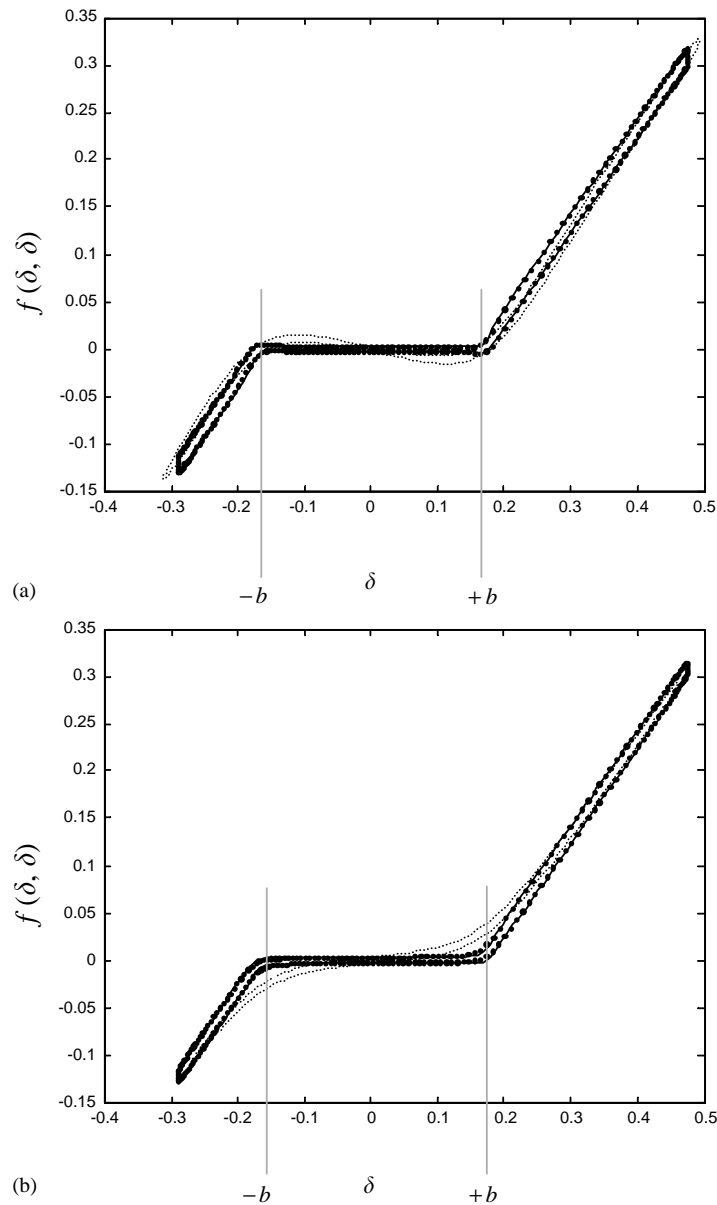

Fig. 9. Effect of the smoothening factor σ on the non-linear function $f(\delta, \dot{\delta})$ for case 2 with $\alpha = 0.00$, $H_1 = 0.005$, and $H_2 = 0.02$. (a) With $\bar{g}_1(\delta)$; (b) with $\bar{g}_2(\delta)$. (–) $\sigma = 100$; (○) $\sigma = 50$; (· · · · ·) $\sigma = 10$.

Significant differences are observed between $\sigma = 10$ and 50 for case 2 with $\alpha = 0.18$. This condition demonstrates strong super-harmonic responses in all approximations. The choice of $\sigma = 10$ does not properly predict the super-harmonic responses, and it generates higher $\delta_{r.m.s.}$ values in $\hat{g}_2$, $\hat{g}_3$, and $\hat{g}_4$. Conversely, $\hat{g}_1$ provides lower $\delta_{r.m.s.}$ values in the super-harmonic regime when $\sigma = 10$. It seems that the employment of $\hat{g}_1$ must be undertaken with some care especially when active super-harmonic responses are present.

The effect of σ value diminishes when the frictional hysteresis is described in the non-linear function. This is shown in Fig. 6, which examines the dual-staged frictional hysteresis for case 2 with $\alpha = 0.00$, $H_1 = 0.005$, and $H_2 = 0.02$. Fig 9 illustrates how this non-linearity is approximated by the smoothening functions. Note that spurious super-harmonic peaks appear when σ is very low; however, such spurious super-harmonic peaks disappear for $\sigma \geqslant 50$. This represents a significant improvement over the results shown in Fig. 4. However, the tendencies of response curves with lower σ values are the same, though with reduced amplitudes. Therefore, a sufficiently large σ is recommended for non-linear analyses.

5. Conclusion

Overall, the σ value affects those frequency response regimes that are influenced by the stiffness transitions. However, the peak values of $\delta_{r.m.s.}$ at resonances appear to be insensitive to the choice of σ. Therefore, $\sigma \geqslant 100$ can be used with an error bound of 5% when compared with an extremely high σ value (say 10^6). The lower σ values should ensure minimal numerical difficulties when solving the non-linear differential equations using the Newton–Raphson method. This means that semi-analytical methods should have no difficulty in evaluating the error residual even when a severe stiffness transition, such as $\alpha = 0$, is encountered. Furthermore, the small differences between the $\hat{g}_1$, $\hat{g}_2$, $\hat{g}_3$ and $\hat{g}_4$ approximations may grow, possibly resulting in a critical numerical overflow problem when the derivatives are required. For example, $\hat{g}'_1$ contains a σ^5 term in Eq. (4c) in contrast with a $1/\sigma$ term for $\hat{g}'_2$ in Eq. (5c). Finally, the non-linear stiffness functions like $\hat{g}_3$, when coupled with friction or impact damping, cannot be applied because of a singularity involved in the sgn function. Further, the localized smoothening function $\hat{g}_4$ provides advantages only in semi-analytical methods. The most suitable functions (such as $\hat{g}_1$ and $\hat{g}_2$) can be employed in both direct time domain numerical integration and semi-analytical methods though these must be handled with some care.

Acknowledgements

References

[1] R. Singh, H. Xie, R.J. Comparin, Analysis of an automotive neutral gear rattle, Journal of Sound and Vibration 131 (1989) 177–196.

[2] R.J. Comparin, R. Singh, Non-linear frequency response characteristics of an impact pair, Journal of Sound and Vibration 134 (2) (1989) 259–290.

[3] C. Padmanabhan, R.C. Barlow, T.E. Rook, R. Singh, Computational issues associated with gear rattle analysis, Journal of Mechanical Design 117 (1995) 185–192.

[4] E. Trochon, R. Singh, Effect of automotive gearbox temperature on transmission rattle noise, Noise-Con 98 Proceedings, 1998, pp. 151–156.

[5] T.C. Kim, R. Singh, Dynamic interactions between loaded and unloaded gear pairs under rattle conditions (Paper no. 2001-01-1553), SAE Transactions, Journal of Passenger Cars: Mechanical Systems 110 (Section 6) (2001) 1934–1943.

[6] C.J. Couderc, J. Der Hagopian, G. Ferraris, Vehicle driveline dynamic behavior: experimentation and simulation, Journal of Sound and Vibration 218 (1) (1998) 133–157.

[7] J.P. March, N.N. Powell, Practical applications of dynamic system modeling in powertrain & vehicle refinement, International Symposium on Vehicle NVH Proceedings, 1996, pp. 297–314.

[8] T.C. Kim, T.E. Rook, R. Singh, Super and sub-harmonic response calculations for a torsional system with clearance non-linearity using the harmonic balance method, Journal of Sound and Vibration, submitted.

[9] C. Padmanabhan, R. Singh, Dynamics of a piecewise non-linear system subject to dual harmonic excitation using parametric continuation, Journal of Sound and Vibration 184 (5) (1995) 767–799.